International Journal of Advance Research and Innovation
Vol. 2(2), Apr-Jun 2014, pp. 167-184
Doi: 10.51976/ijari.221424
www.gla.ac.in/journals/ijari
© 2014 IJARI, GLA University

**Article Info**
Received: 02 Mar 2014 | Revised Submission: 10 Apr 2014 | Accepted: 20 May 2014 | Available Online: 15 Jun 2014

# Performance Evaluation of Vapour Compression Refrigeration System using Eco Friendly Refrigerants in Primary Circuit and Nanofluid (Water-Nano Particles Based) in Secondary Circuit

*R. S. Mishra**

**ABSTRACT**

*This paper describes thermal modeling of Vapor Compression Refrigeration System using R134a in primary circuit and AL2O3-Water based nanofluids in secondary circuit. The model uses information of the secondary fluids input conditions geometric characteristics of the system, size of nanoparticles and the compressor speed to predict the secondary fluids output temperatures, the operating pressures, the compressor power consumption and the system overall energy performance. Such an analysis can be conveniently useful to compare the thermal performance of different nano particles (Cu, Al2o3, Tio2 and CuO) based nano fluid as a secondary fluid in a Vapor Compression Refrigeration System. The influence of input variables on the output of the system is presented. Such a model can also be used to design various Components viz. Evaporator, Compressor, Condenser and Throttle Valve for Vapor Compression Refrigeration Systems for any desired cooling capacity. The use of nanofluids as a secondary fluid in vapour compression refrigeration systems was studied and computational simulation program was developed to solve the non linear equations of the system model. Simulation results have shown that for the same geometric characteristics of the system performance increased from 17% to 20% by application of nanofluid as a secondary fluid in VCS.*

***Keywords:*** *Sustainable Technologies; Sustainable Development; Green Technologies; Alternative Refrigerants; Eco Friendly Refrigerants; Energy Exergy Analysis; Irreversibility Analysis.*

## 1.0 Introduction

Refrigeration is a technology which absorbs heat at low temperature and provides temperature below the surrounding by rejecting heat to the surrounding at higher temperature. Simple vapour compression refrigeration system which consists of four major components compressor, expansion valve, condenser and evaporator in which total cooling load is carried at one temperature by single evaporator but in many applications like large hotels, food storage and food processing plants, food items are stored in different compartment and at different temperatures. Therefore there is need of multi evaporator vapour compression refrigeration system. The systems under vapour compression technology consume huge amount of electricity, this problem can be solved by improving performance of system. Performance of systems based on vapour compression refrigeration technology can be improved by following:

1. The performance of refrigerator is evaluated in term of COP which is the ratio of refrigeration effect to the net work input given to the system. The COP of vapour compression refrigeration system can be improved either by increasing refrigeration effect or by reducing work input given to the system.
2. It is well known that throttling process in VCR is an irreversible expansion process. Expansion process is one of the main factors responsible for exergy loss in cycle performance because of entering the portion of the refrigerant flashing to vapour in evaporator which will not only reduce the cooling capacity but also increase the size of evaporator. This problem

**Department of Mechanical & Production Engineering, Delhi Technological University, New Delhi, India*
*(E-mail: professor-rsmishra@yahoo.co.in)*

3. can be eliminated by adopting multi-stage expansion where the flash vapours is removed after each stage of expansion as a consequence there will be increase in cooling capacity and reduce the size of the evaporator.

**1.1 Literature review**

Kumar et al. (1989) carried out energy and exergy analysis of vapour compression refrigeration system by using exergy-enthalpy diagram. For calculating the coefficient of performance, they had done first law analysis (energy analysis) and for evaluation of various losses occurred in different components they used R11 and R12 as refrigerants in the exergy analysis of vapour compression cycle.

Nikolaidis and Probert (1998) suggested that there is need for optimizing the conditions imposed upon the condenser and evaporator by detailed analytical studied for finding the plant irreversibility by changing evaporator and condenser temperatures of two stage vapour compression refrigeration plant using R22. Yumrutas et al. (2002) considered the exergy analysis based investigation of effect of condensing and evaporating temperature on vapour compression refrigeration cycle in terms of pressure losses, COP, second law efficiency and exergy losses and found that the variation in condenser temperature and evaporator temperature have negligible effect on exergy losses of compressor and expansion valve, and investigated first law efficiency and exergetic efficiency increase and total exergy losses in the vapour compression system decrease with increase in evaporator and condenser temperature.

Halimic et al. (2003) studied the thermodynamic performance of R401A, R290 and R134A with R12 in the vapour compression refrigeration system, which was originally designed for R12 and found R134A can be replaced in the same system without any medication in the system components due to similar performance of R134a in comparison with R12. They also suggested that in reference to green house impact the hydrocarbon R290 presented best results in comparison of above refrigerants.

Xuan and Chen (2004) found the HFC-161 as the replacement of R502 through experimental investigation and also observed that HFC-161 gives same and higher performance than R404A at lower and higher evaporative temperature respectively by designing vapour compression refrigeration system for R404A.

Cabello et al. (2004) studied experimentally the effect of condensing pressure, evaporating pressure and degree of superheating on the single stage vapour compression refrigeration system using R22, R134a &R407C and found that mass flow rate is greatly affected by change in suction conditions of compressor due to refrigeration capacity because refrigeration capacity depended on mass flow rate through evaporator. They also observed that for higher compression ratio R22 gives lower COP than R407C.

Spatz and Motta (2004) studies mainly focused on replacement of R12 with R410a through experimental investigation of medium temperature vapour compression refrigeration cycles.and comparison was made in terms of heat transfer and pressure drop characteristics and found the R410a gives best performance among R12, R404a and R290a.

Han et al. (2007) observed in the different working conditions through experimental investigation that there could be replacement of R407C in vapour compression refrigeration system having rotor compressor with mixture of R32/R125/R161 showing higher COP, less pressure ratio and slightly high discharge compressor temperature without any modification in the same system.

Cabello et al. (2007) had studied about the effect of operating parameters on COP, work input and cooling capacity of single-stage vapour compression refrigeration system and found a great influence on energetic parameters due change in suction pressure, condensing and evaporating temperatures.

Arora and Kaushik (2008) developed numerical model of actual vapour compression refrigeration system with liquid vapour heat exchanger and did energy and exergy analysis on the same in the specific temperature range of evaporator and condenser. They concluded that R502 is the best refrigerant compare to R404A and R507A, compressor is the worst and liquid vapour heat exchanger is best component of the system.

Getu and Bansal (2008) had optimized the design and operating parameters of like condensing temperature, subcooling temperature, evaporating

temperature, superheating temperature and temperature difference in cascade heat exchanger R744-R717 cascade refrigeration system. A regression analysis was also done to obtain optimum thermodynamic parameters of same system.

Mohanraj et al. (2009) conducted experiment on domestic refrigerator and observed that under different environmental temperatures COP of system using mixture of R290 and R600a in the ratio of 45.2: 54.8 by weight showing up to 3.6% greater than same system using R134a, also discharge temperature of compressor with mixture of R290 and R600a is lower in the range of 8.5-13.4K than same compressor with R134a.

Padilla et al. (2010) studied exergy analysis of domestic vapour compression refrigeration system with R12 and R413A and concluded that performance in terms of power consumption, irreversibility and exergy efficiency of R413A is better than R12, so R12 can be replaced with R413A in domestic vapour compression refrigeration system.

Stanciu et al. (2011) conducted the numerical and graphical investigation on one stage vapour compression refrigeration system for studied refrigerants (R22, R134a, R717, R507a, R404a) in terms of COP, compressor work, exergy efficiency and refrigeration effect. They also studied the effect of subcooling, superheating and compression ratio on the same system using considered refrigerants and present system optimization when working with specific refrigerant.

Ahamed et al. (2011) emphasized on use of hydrocarbons and mixture of hydrocarbons and R134a in vapour compression refrigeration system and observed that compressor shows much higher exergy destruction as compared to rest of components of vapour compression refrigeration system and this exergy destruction can be minimized by using of nanofluid and nanolubricants in compressor.

Bolaji et al. (2011) had done comparative analysis of R32, R152a and R134a refrigerants in vapour compression refrigerator through experimental investigation and found that R32 refrigerant gives lowest performance and R134a and R152a showing nearly same performance but best performance was obtained of system using R152a.

Ahamed et al. (2012) had performed experimental investigation of domestic refrigerator with hydrocarbons (isobutene and butane) by energy and exergy analysis. They reached to the results that energy efficiency ratio of hydrocarbons comparable with R134a but exergy efficiency and sustainability index of hydrocarbons much higher than that of R134a at considered evaporator temperature. It was also found that compressors shows highest system defect (69%) among components of considered system.

Anand and Tyagi (2012) did detailed exergy analysis of 2TR window air conditioning test rig with R22 as working fluid and reached to the conclusions that irreversibility in system components will be highest when the system is 100% charged and lowest when 25% charged and irreversibility in compressor is highest among system components.

Reddy et al. (2012) did numerical analysis of vapour compression refrigeration system using R134a, R143a, R152a, R404A, R410A, R502 and R507A and discussed the effect of evaporator temperature, degree of subcooling at condenser outlet, superheating of evaporator outlet, vapour liquid heat exchanger effectiveness and degree of condenser temperature on COP and exergetic efficiency.

They reported that evaporator and condenser temperature have significant effect on both COP and exergetic efficiency and also found that R134a has the better performance while R407C has poor performance in all respect.

Selladurai and Saravanakumar (2013) compared the performance between R134a and R290/R600a mixture on a domestic refrigerator which is originally designed to work with R134a and found that R290/R600a hydrocarbon mixture showed higher COP and exergetic efficiency than R134a. In their analysis highest irreversibility obtained in the compressor compare to condenser, expansion valve and evaporator.

Mastani Joybari et al. (2013) performed experimental investigation on a domestic refrigerator originally manufactured to use of 145g of R134a.

They concluded that exergetic defect occurred in compressor was highest as compare to other components and through their analysis it has been found that instead of 145g of R134a if 60g of R600a is used in the considered system gave same performance which ultimately result into economical advantages and reduce the risk of flammability of hydrocarbon refrigerants.

Elcock (2007) observed that TiO2 nanoparticles can be used as additives to enhance the solubility of the mineral oil with the hydrofluorocarbon (HFC) refrigerant. They also observed that refrigeration systems using a mixture of HFC134a and mineral oil with TiO2 nanoparticles appear to give better performance by returning more lubricant oil to the compressor with similar performance to systems using HFC134a and POE oil.

Hindawi (2009) carried out an experiment on the boiling heat transfer characteristics of R22 refrigerant with Al2O3 nanoparticles and observed that the nano particles enhanced the refrigerant heat transfer characteristics with reduced bubble sizes.

Eastman et al. (1996) found the pool boiling heat transfer characteristics of R11 refrigerant with TiO2 nanoparticles and showed that the heat transfer enhancement reached 20% at a particle loading of 0.01 g/L.

Liu et al. (2006) studied ed the effects of carbon nanotubes (CNTs) on the nucleate boiling heat transfer of R123 and HFC134a refrigerants and observed that that CNTs increase the nucleate boiling heat transfer coefficients for these refrigerants. Authors noticed large enhancements of up to 36.6% at low heat fluxes of less than 30 kW/m2. Thus, the use of nanoparticles in refrigeration systems is a new, innovative way to enhance the efficiency and reliability in the refrigeration system.

Jiang et al. (2009) observed experimentally the thermal conductivities of carbon nanotube (CNT) nanorefrigerants are much higher than those of CNT–water nanofluids or sphericalnanoparticle–R113 nanorefrigerant and found that the smaller the diameter of CNT larger the thermal conductivity enhancement of CNT nanorefrigerant.

Hwang et al. (2006) found the thermal conductivity enhancement of nanofluids is greatly influenced by thermal conductivity of nanoparticles and basefluid. They observed the thermal conductivity of water based nanofluid with multiwall carbon nano tube has noticeably higher thermal conductivity compared to SiO2 nanoparticles in the same base fluid.

Yoo et al. (2007) observed that surface to volume ratio of nanoparticles is a dominant factor that influences the nanofluids thermal conductivity rather than nanoparticles thermal conductivity. Surface to volume ratio is increased with smaller sizes of nanoparticles.

Choi et al. (2001) found 150% thermal conductivity enhancement of poly (a-olefin) oil with the addition of multiwalled carbon nanotubes (MWCNT) at 1% volume fraction.

Yang (2006) found 200% thermal conductivity enhancement for poly (a-olefin) oil containing 0.35% (v/v) MWCNT. They observed the thermal conductivity enhancement was accompanied by a three order of magnitude increase in viscosity.

Eastman et al. (2001) observed 40% thermal conductivity enhancement for ethylene glycol with 0.3% (v/v) copper nano particles (10 nm diameter) by added about 1% (v/v) thioglycolic acid to aid in the dispersion of the nano particles and observed that yielded a greater thermal conductivity than the same concentration of nanoparticles in the ethylene glycol without the dispersant.

Jana et al. (2006) measured the thermal conductivity of a similar copper containing nanofluid, except the base fluid was water and laurate salt was used as a dispersant and found the 70% thermal conductivity enhancement for 0.3% (v/v) cu nanoparticles in water.

Kang et al. (2006) observed a 75% thermal conductivity enhancement for ethylene glycol with 1.2% (v/v) diamond nanoparticles between 30 and 50 nm in diameter by measuring the thermal conductivity of nanofluids and have found no anomalous results.

Lee et al. (2008) found the thermal conductivity of nanofluids is affected by pH level and addition of surfactant during nanofluids preparation stage. It was observed that better dispersion of nanoparticles is achieved with addition of surfactant such as sodium dodecylbenzenesulfonate and found that the optimum combination of pH and surfactant leads to 10.7% thermal conductivity enhancement of 0.1% Cu/H2O nanofluids.

Jiang et al. (2009) observed that thermal conductivity of nanofluids also depend on the nanoparticles size and temperature.

Wu et al. (2008) observed that the pool boiling heat transfer was enhanced at low nanoparticles concentration of TiO2 in R11 but deteriorated under the condition of high nanoparticles concentration.

Trisaksri and Wongwises (2009) investigated TiO2 in HCFC 1416 in a cylindrical copper tube and found that the nucleate pool boiling heat transfer deteriorated with increasing nanoparticle concentrations especially at higher heat fluxes.

Hao et al. (2009) investigated the heat transfer characteristics of refrigerant-based nanofluids flow boiling inside a smooth tube at different nanoparticles concentration, mass fluxes, heat fluxes, and inlet vapor qualities to analyze the influence of nanoparticles on the heat transfer characteristics of refrigerant-based nanofluid flow boiling inside the smooth tube and developed correlation for predicting the heat transfer coefficient of refrigerant-based nanofluid and the predicted heat transfer coefficients agree with 93% of the experimental data and found that the heat transfer coefficient of refrigerant-based nanofluid in flow boiling is larger than that of pure refrigerant and the maximum enhancement is about 29.7% when observed with a mass fraction of nanoparticles 0–0.5 wt%. and the reduction of the boundary layer height due to the disturbance of nanoparticles enhances the heat transfer.

Hao et al. (2010) observed experimentally the nucleate pool boiling heat transfer characteristics of refrigerant/oil mixture with diamond nanoparticles. The refrigerant was R113 and the oil was VG68. The results indicate that the nucleate pool boiling heat transfer coefficient of R113/oil mixture with diamond nanoparticles is larger than that of R113/oil mixture by maximum of 63.4% and the enhancement increases with the increase of nanoparticles concentration in the nanoparticles/oil suspension and decreases with the increase of lubricating oil concentration.

Authors developed a correlation for predicting the nucleate pool boiling heat transfer coefficient of refrigerant/oil mixture with nanoparticles and it agrees well with the experimental data of refrigerant/oil mixture with nanoparticles.

Wang et al. (2006) conducted experimental study of the boiling heat transfer characteristics of R22 refrigerant with Al2O3 nanoparticles and observed that the nanoparticles enhanced the refrigerant heat transfer characteristics with reduced bubble sizes that moved quickly near the heat transfer surface.

Li et al. (2006) studied the pool boiling heat transfer characteristics of R11 refrigerant with TiO2 nanoparticles and showed that the heat transfer enhancement reached 20% at aparticle loading of 0.01 g/L.

Peng et al. (2009) studied the influence of nanoparticles on the heat transfer characteristics of refrigerant-based nanofluids flow boiling inside a horizontal smooth tube, and developed a correlation for predicting heat transfer performance of refrigerant based nanofluids by preparing refrigerant based nanofluids, In the experiment, R113 refrigerant and CuO nanoparticles were used and found that the heat transfer coefficient of refrigerant-based nanofluids is higher than that of pure refrigerant, and the maximum enhancement of heat transfer coefficient found to be about 29.7%.

Kumar and Elansezhian (2014) experimentally investigated the effect of concentration of nano Zno ranges in the order of 0.1%,0.3% and 0.5% v with particle size of 50 nm on various thermodynamic parameters (i.e. COP, suction temperature ,input power and pressure raio with 152a as working fluid.In simple vapour compression refrigeration system.

They found that maximum COP of 3.56 and 21% reduction of power input was obtained with 0.5% v of Zno .Pressure ratio decreases with increase in nano Zno concentration.

Mahbubul et al. (2013) Thermo-physical properties, pressure drop and heat transfer performance of Al2O3 nanoparticles suspended in the ecofriendly R-134a refrigerant was investigated .To determine the thermal conductivity and viscosity of the nano refrigerants for the nanoparticle concentrations of 1 to 5 vol.% existing model was studied .Thermal conductivity of Al2O3/R-134a nanorefrigerant increased with the augmentation of particle concentration and temperature however, decreased with particle size intensification.

In addition, the results of viscosity, pressure drop, and heat transfer coefficients of the nanorefrigerant show a significant increment with the increase of volume fractions.

The frictional pressure drop shows rapid increment of more than 3 vol. % with particle volume fraction, and the pumping power increases with particle concentration similar to pressure drop increment.

The pumping power is proportional to the pressure drop of nano-refrigerant.

**1.2 Research gaps identified**

Based on the literature it was observed that Researchers have gone through detailed first law analysis in terms of coefficient of performance and second law analysis in term of exergetic efficiency of simple vapour compression refrigeration system with single evaporator.

Authors also analyzed the effect of nanofluids on simple vapour compression cycle in the term of pool boiling, COP, Thermal conductivity etc Researchers did not go through irreversibility analysis or second law analysis of multiple evaporators systems with multi-stage expansion in vapour compression refrigeration systems.

Researchers did not go through irreversibility and second law analysis of single and multi-stage vapour compression refrigeration systems by using of nanofluid.

**1.3 Research objectives**

1. Detailed theoretical analysis in terms of first law efficiency, second law efficiency, and exergy destruction of single and multiple stages vapour compression refrigeration systems using ecofriendly refrigerants.
2. Detailed system optimization to be done and experimental test rig to be developed to verify theoretical and experimental work.
3. Effect of nanofluids on first law efficiency, second law efficiency and irreversibility of each component of both systems (single and multi-stage VCR) experimentally.

**1.4 Methods for performance improvements**

To improve thermal performance of vapour compression refrigeration systems (both single and multiple evaporator system) by improving:

First law efficiency-According to first law of thermodynamic energetic efficiency /COP is defined as the ratio of net refrigeration effect to the per unit power consumed.

First law analysis restricted to calculate only coefficient of performance of the systems and Second law efficiency- The concept of exergy was given by second law of thermodynamics.

Second law efficiency is the exergy of the heat abstracted in to the evaporators from the space to be cooled and exergy of fuel is actual compressor work input.

Reduction of system defect by using of nanoparticles in vapour compression refrigeration systems which results into reduction of work input.

**1.5 Methodology**

To obtain above research objectives following methodology have to be adopted:

Fabrication of multi and single stage vapour compression systems Verification of theoretical results with results obtained from experimental setup. Analysis in terms of energy efficiency, exergetic efficiency and irreversibility of each component of both (single and multi stage vapour compression) systems with pure refrigerant (R-134a). Effect on above parameters with nanofluids.

**2.0 Model Description**

The general structure of the proposed model is presented in Fig. 1., where it can be seen that the model inputs are the secondary fluids/ nanofluid input variables and the compressor speed, neglecting sub-cooling degree at the condenser outlet and superheating degree at the evaporator outlet, for simplicity.

Using these inputs and the main characteristics of the compressor and heat exchangers, the model predicts the operating pressures (without considering pressure drops), secondary fluids output variables and the energy performance. in both condenser & evaporator is counter flow.

In the evaporator Refrigerant flows inside the inner tube and nanofluid surrounding the inner tube and the condenser water flows inside the inner tube and refrigerant surrounding the inner tube.

The model computes the refrigerant properties and the thermo-physical properties of secondary fluids are evaluated by using Engineering equation solver *(EES).*

The model consists of a set of five equations based on physical laws describing the main parts of the system, as shown schematically in Fig. 1.

There frigerant states are numbered in Fig. 1.3 The refrigerant mass flow rate *(mr)* has been modeled using Eq. (1), where the compressor volumetric efficiency ($\eta v$) has been expressed as a function of operating pressure and compressor speed

(*N*) as shown in Eq. (2). For simplicity, *(ρ1)* is the refrigerant density considered is the one corresponding to the saturated vapor at the evaporating pressure and *Vg* is the geometric compressor volume.

**Fig 1: Schematic Structure of Model**

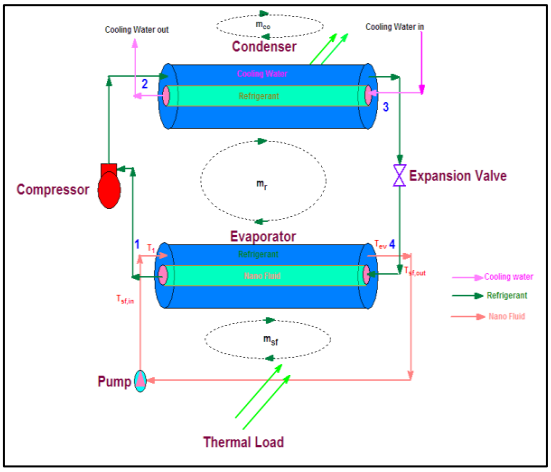


**Fig 2: Vapour Compression cycle**

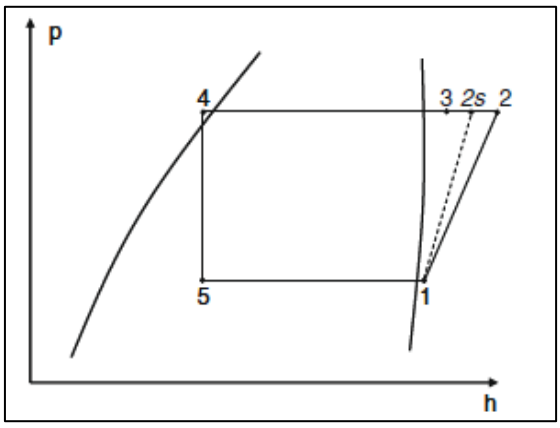


The model consists of a set of five equations based on physical laws describing the main parts of the system, as shown schematically in Fig. 2. The refrigerant states are numbered in Fig. 1.3. The refrigerant mass flow rate *(mr)* has been modeled using Eq. (1), where the compressor volumetric efficiency (*ηv*) has been expressed as a function of operating pressure and compressor speed (*N*) as shown in Eq. (2). For simplicity, *(ρ1)* is the refrigerant density considered is the one corresponding to the saturated vapor at the evaporating pressure and *Vg* is the geometric compressor volume.

$$m_r = \eta_v \cdot \rho_1 \cdot V_g \cdot N \tag{1}$$

$$\eta_v = 0.73341 - 0.00003062 \cdot N + 0.04561 \cdot P_e - 0.01237 \cdot P_k \tag{2}$$

Where, $P_k$ & $P_e$ is the condenser and evaporator pressure respectively.

## 2.1 Evaporator Formulation

The evaporator is modeled using two equations, one based on the heat exchanger energy balance,

$$m_r \cdot (h_1 - h_5) = m_b \cdot Cp_b \cdot (Tb_{in} - Tb_{out}) \tag{3}$$

Where, $h_1$ and $h_5$ is the enthalpy at state 1 and 5 of refrigerant, see Fig. 3.3 $Cp_b$ is the Specific heat of brine. $Tb_{in}$ and $Tb_{out}$ is the inlet and outlet Temperature of the brineThe other making use of the logarithmic mean temperature difference and the global heat transfer coefficient, with a LMTD correction factor equal to1

$$m_r \cdot (h_1 - h_5) = U_e \cdot S_e \cdot \left[ \frac{Tb_{in} - T_e - (Tb_{out} - T_e)}{\ln\left(\frac{Tb_{in} - T_e}{Tb_{out} - T_e}\right)} \right] \tag{4}$$

Where, $U_e$ is the evaporator global heat transfer. $S_e$ is the surface area of the evaporator. $T_e$ is the evaporator Temperature. The evaporator global heat transfer coefficient *(Ue)* used in Eq. *(4)* is computed as:

$$U_e = \frac{1}{r_o} \cdot \left[ \frac{1}{\alpha_b \cdot r_o} + \frac{\ln\left(\frac{r_o}{r_i}\right)}{K_M} + \frac{1}{\alpha_w \cdot r_i} + R_{TFO} \right]^{-1} \tag{5}$$

**Where**,
$K_M$ is the thermal conductivity of Metal.
$r_i$ & $r_o$ is the outside and inside radius of the tube.
$\alpha_{lv}$ is the heat transfer coefficient for the refrigerant.
$R_{TFo}$ is the thermal resistance associated to the fouling in the heat exchanger tubes ($R_{T\ Fo}$ = 0.000086 $m^2$ K/W, manufacturer data for water/water).

The heat transfer coefficient for the brine *($\alpha_b$)* is computed using the Zukauskas' correlation.

$$\alpha_b = \frac{K_b}{D_o} \cdot C_1 \cdot Re_b^{m_1} \cdot Pr_b^{0.36} \cdot \left[ \frac{\mu_b}{\mu_{bM}} \right]^{0.25} \tag{6}$$

**Where**,
$K_b$ is the thermal conductivity of brine.

$D_O$ is the outer diameter of tube.
$Re_b$ is the Reynold's No. of brine.
$Pr_b$ is the Prandle No. of brine.
$C_1$ and $m_1$ is a coefficient of the correlation.
$\mu_b$ viscosity of brine.
$\mu_{bM}$ viscosity of brine at metal temperature.
While the refrigerant heat transfer coefficient $(\alpha_{lv})$ is computed With the Chen's correlation.

$$\alpha_{lv} = sf \cdot \alpha_{nb} + F \cdot \alpha_{conv} \quad (7)$$

**Where**,
$\alpha_{nb}$ is the nucleated boiling component obtained using Foster–Zuber correlation.
$\alpha_{conv}$ is the convective component, computed using the Dittus–Boelter correlation.
$sf$ is the suppression factor.
$F$ is the Reynolds number factor.
The values of these parameters are computed using the following equations:

$$\alpha_{nb} = 0.00122 \cdot \frac{K_{Le}^{0.79} \cdot Cp_{Le}^{0.45} \cdot \rho_{Le}^{0.49}}{\sigma^{0.5} \cdot \mu_{Le}^{0.29} \cdot \lambda_e^{0.24} \cdot \rho_{ve}^{0.24}} \cdot \delta T_{sat}^{0.24} \cdot \delta P_{sat}^{0.75} \quad (8)$$

**Where**,
$\sigma$ is the surface tension of refrigerant.
$K_{Le}$ is the thermal conductivity of refrigerant in liquid phase in evaporator.
$Cp_{Le}$ is the specific heat of refrigerant in liquid phase in evaporator.
$\rho_{ve}$ & $\rho_{Le}$ is the density of refrigerant in vapor and liquid phase in evaporator.
$\lambda_e$ is the latent heat in evaporator.

$$\alpha_{conv} = 0.023 \cdot Re^{0.8} \cdot Pr^{0.4} \cdot \frac{K_L}{D_i} \quad (9)$$

$$sf = \frac{1}{(1 + 0.00000253) \cdot (Re \cdot F^{1.15})^{1.17}}$$

$$F = \begin{cases} 1 & 1/X_{tt} < 0.1 \\ 2.35\,(1/X_{tt} + 0.213)^{0.736} & 1/X_{tt} > 0.1 \end{cases}$$

**Where**,
$D_i$ is the coil inner diameter.
$X_{tt}$ is the Martinelli's Parameter.
$X_v$ is the quality of refrigerant.

$$X_{tt} = \left[\frac{1 - X_v}{X_v}\right]^{0.9} \cdot \left[\frac{\rho_v}{\rho_L}\right]^{0.5} \cdot \left[\frac{\mu_L}{\mu_v}\right]^{0.1}$$

**2.2 Compressor formulation**

The compressor behavior is modeled from the isentropic efficiency *(ηis)* and the working pressures. Thus, from the refrigerant state at the evaporator outlet, the refrigerant state at the compressor discharge is determined using Eq.*(10)* from the isentropic compression work and the compression isentropic efficiency,

$$h_2 = h_1 + \frac{h_{2s} - h_1}{\eta_{is}} \quad (10)$$

where, $\eta_{is}$ is the compression isentropic efficiency and it has been obtained from gathered empirical data, as a function of operating pressures, yielding Eq. *(11)*

$$\eta_{is} = 0.156323 + 0.0000912 \cdot N + 0.004302 \cdot P_k + 0.09151 \cdot P_e \quad (11)$$

In order to compute the compressor power consumption, the model makes use of a global electromechanical efficiency (12) fitted with the empirical data as a function of *N*,

$$\eta_g = 0.00002805 \cdot N^2 + 0.02593961 \cdot N + 6.4965 \quad (12)$$

As in the case of Eq.(2) the efficiencies given by Eq. (11) and (12) Show a significant relationship among the variables with a confidence level of 99%.

The correlations for isentropic and electromechanical efficiency are fitted for the compressor used in the facility, and similar relations should be obtained from experimental results for another compressor.

The heat transfer from the refrigerant at the compressor discharge line to the condenser inlet has been modeled, due to the considerable length of the line in the experimental chiller facility, using expression (13)

$$\dot{m}_r \cdot (h_2 - h_3) = U_{23} \cdot S_{23} \cdot \left[\frac{T_2 - T_{air} - (T_3 - T_{air})}{\ln\left(\frac{T_2 - T_{air}}{T_3 - T_{air}}\right)}\right] \quad (13)$$

$U_{23}$ is the global heat transfer coefficient used in Eq. (11) is computed as:

$$U_{23} = \frac{1}{r_o} \cdot \left[\frac{1}{\alpha_i \cdot r_i} + \frac{\ln\left(\frac{r_o}{r_i}\right)}{K_M} + \frac{1}{\alpha_o \cdot r_o}\right]^{-1} \quad (14)$$

Using a modified version of the Gnielinski's correlation (14a) for the refrigerant inside the tubes, $\alpha_i$.
If Re < 10000 then use,

$$\alpha_i = \frac{K_v}{2 \cdot r_i} \cdot \left[ \frac{\frac{Fric}{8} \cdot (Re - 1000) \cdot Pr}{1 + 12.7 \cdot \left(\frac{Fric}{8}\right)^{0.5} \cdot (Pr^{(2/3)} - 1)} \right] \cdot \left[\frac{\mu_v}{\mu_{vM}}\right]^{0.11} \quad (14a)$$

Or, If Re >10000 then use,

$$\alpha_i = \left[\frac{K_v}{2 \cdot r_i}\right]^{0.027} \cdot Re^{(4/5)} \cdot Pr^{(1/3)} \cdot \left[\frac{\mu_v}{\mu_{vM}}\right]^{0.14} \quad (14b)$$

**Where,**

$$Fric = \frac{1}{(0.79 \cdot \ln(Re) - 1.64)^2}$$

and the natural-convection heat transfer coefficient is computed as,

$$\alpha_o = \frac{K_{air}}{D_o} \cdot (Nul^{10} + Nutt^{10})^{\left[\frac{1}{10}\right]} \quad (15)$$

**Where,**

$$Nul = 2 \cdot \frac{fc}{\ln\left[1 + \frac{2 \cdot fc}{NuT}\right]}$$

$$Nutt = 0.103 \cdot Ra^{(1/3)}$$

Being

$$NuT = 0.7772 \cdot 0.103 \cdot Ra^{0.25}$$

$$F = 1 - \frac{0.13}{NuT^{0.16}}$$

$$Ra = g \cdot \frac{1}{T_{air}} \cdot (T_M - T_{air}) \cdot \frac{(2 \cdot r_0)^3}{\frac{\mu_{air} \cdot K_{air}}{\rho_{air} \cdot \rho_{air} \cdot Cp_{air}}} \quad (16)$$

### 2.3 Condenser formulation

The condenser behavior is modeled by dividing the heat exchanger into two zones the superheated vapor zone and the condensing zone, assuming no sub-cooling at the condenser outlet, as it has been stated in the assumptions. The overall heat exchanger is then modeled with two energy balances, one using the secondary fluid heat flow rate (17),

$$\dot{m}_r \cdot (h_3 - h_{Vsat}) = m_w \cdot Cp_w \cdot (Tw_{out} - Tw_m) \quad (17)$$

and the other making use of the global heat transfer coefficient *(18)* and assuming a LMTD correction factor equal to 1 for simplicity,

$$\dot{m}_r \cdot (h_3 - h_{Vsat}) = U_v \cdot S_v \cdot \left[\frac{T_k - Tw_m - (T_3 - Tw_{out})}{\ln\left(\frac{T_k - Tw_m}{T_3 - Tw_{out}}\right)}\right] \quad (18)$$

Being *UK* an average heat transfer coefficient computed as,

$$U_k = \frac{U_v \cdot S_v + U_{vl} \cdot (S_k - S_v)}{S_k} \quad (19)$$

Where,

*SK* is the overall heat transfer area of the heat exchanger.

*SV* is the theoretical heat transfer area dedicated to the superheated vapor zone.

$$S_{vL} = S_k - S_v \quad (20)$$

$$\dot{m}_r \cdot (h_{Vsat} - h_{Lsat}) = m_w \cdot Cp_w \cdot (Tw_m - Tw_{in}) \quad (21)$$

$$\dot{m}_r \cdot (h_{Vsat} - h_{Lsat}) = U_{vl} \cdot S_{vL} \cdot \left[\frac{T_k - Tw_m - (T_k - Tw_{in})}{\ln\left(\frac{T_k - Tw_m}{T_k - Tw_{in}}\right)}\right] \quad (22)$$

In the calculation of the partial heat transfer coefficients, $U_V$ and $U_{VL}$, the convection heat transfer coefficient in the water side is computed using Eq. *(14)*. For the computation of the convection heat transfer coefficient associated to the refrigerant one can distinguish between the convection heat transfer coefficient in the superheated vapor zone, given by,

$$\alpha_v = \frac{K_v}{D_o} \cdot C_1 \cdot Re^{m_1} \cdot Pr^{0.36} \cdot \left[\frac{\mu_v}{\mu_{vM}}\right]^{0.25} \quad (23)$$

Where, $C_1$ and $m_1$ depend on the Reynolds number value,

$$[C_1, m_1] = \begin{cases} [0.9, 0.4] & Re \le 100 \\ [0.683, 0.466] & 100 < Re \le 1000 \\ [0.4, 0.6] & 1000 < Re \le 200000 \\ [0.022, 0.84] & Re > 200000 \end{cases}$$

and the convection heat transfer coefficient in the condensing zone, that is computed as,

$$\alpha_k = 0.729 \cdot \left[ \frac{g \cdot \rho_L \cdot (\rho_L - \rho_v) \cdot \lambda_{k,mod} \cdot K_l^3}{\mu_l \cdot T_{abs} \cdot 2 \cdot r_o} \right]^{0.25} \quad (24)$$

Being $\lambda_K$ mod the modified latent heat with the effects of thermal advection,

$$\lambda_{k,mod} = \lambda_k \cdot (1 + 0.68 \cdot j_a) \quad (25)$$

Where,

$$\lambda_k = h_3 - h_{Vsat}$$

and $J_a$ is the Jacobsen's number.

$$j_a = \frac{Cp_L \cdot T_{abs}}{\lambda_k} \quad (26)$$

And

$$T_{abs} = |T_k - T_M \quad (27)$$

Finally, the model consists of a set of nonlinear equations, basically defined by Eqs. *(3), (4), (13), (17),* and *(18),* which constitute a system relating the model output variables, $T_{b,out}$, $T_{w,out}$, $p_e$, $p_k$ and $T_3$, in terms of the model input variables, $m_b$, $m_w$, $T_{b,in}$, $T_{w,in}$ and $N$.

### 2.4 Nanofluid

Nanofluid always be treated as a homogenous fluid. [8] Velagapudi *et al.* (2008) proposed the following correlation for the thermal conductivity of nanofluids

$$\frac{k_{nf}}{K_m} = c \cdot Re_m^{0.175} \cdot \phi_p^{0.05} \cdot \left[ \frac{K_p}{K_m} \right]^{0.2324} \quad (28)$$

Where the Reynolds number is given by

$$Re_m = \frac{1}{V_m} \cdot \left[ \frac{18 \cdot K_p \cdot T}{3.14 \cdot \rho_p \cdot d_p} \right]^{(1/2)} \quad (29)$$

Constant *c* depends on the particle-base fluid combination (Velagapudi *et al.*, 2008). For water-based nanofluids with nanoparticles of Al2O3, CuO, Cu and TiO2, the value of *c* is 1, 1.298, 0.74 and 1.5, respectively.

Concerning viscosity, specific correlations for each nanofluid were employed. For example, for water-Al2O3 nanofluid, the viscosity is given by Pak and Cho (1998), as follows

$$\mu_{nf} = \mu_m \cdot (533.9 \cdot \phi_p^2 + 39.11 \cdot \phi_p + 1) \quad (30)$$

Finally, density and specific heat are determined based on mass and energy balances, respectively.

$$\rho_{nf} = \rho_p \cdot \phi_p + \rho_m \cdot (1 - \phi_p) \quad (31)$$

$$c_{p,nf} = \frac{\phi_p \cdot \rho_p \cdot c_{p,p} + (1 - \phi_p) \cdot \rho_m \cdot c_{p,m}}{\rho_{nf}} \quad (32)$$

## 3.0 Results and Discussions

### Cycle calculation and solution method

Input date for the thermal modeling included the geometry of compressor and heat exchangers (inner and outer diameters), refrigerant type, nanofluid characteristics(base fluid and nanoparticle material, size and volume fraction), inlet temperatures of condenser coolant (Water) and secondary fluid (nanofluid), condensing and evaporating temperatures, excluding superheating in the evaporator and subcooling in the condenser thermal load. The resulting system of equations was solved in the EES (Engineering Equation Solver) platform. Simulation main results include

(i) Performance parameter of the thermal model for different types of eco friendly refrigerant without nanofluid

(ii) Performance parameter of the thermal model for different types of eco friendly refrigerant with nanofluid and % enhancement of first law of thermodynamics.

Table-1 to 12 showing the effect of evaporator temperature with performance parameters. As evaporator temperature increases, the first law efficiency of vapour compression refrigeration system is increases. Also second law efficiency is also increases up to variation of evaporator temperature of -5oC and then decreases. Therefore optimum temperature of evaporator is found to be -5oC. Similarly exergy destruction ratio is also decreases up to 273K and then increases.

The optimum evaporator temperature to be found to be 273K for optimum EDR. Table-13 to 24 showing the effect of condenser temperature with performance parameters. As condenser temperature increases, the first law efficiency of vapour compression refrigeration system is decreases. Also second law efficiency is also decreases.. Similarly exergy destruction ratio is also decreases.

**Table 1: Variation of Performance Parameters With Evaporator Temperature in the Vapour Compression Refrigeration System using R-125 In Primary Circuit and Titanium Dioxide Nonoparticles of 10 Micron Particle's Diameter in Secondary Circuit for Condenser Temperature 48oc**

| $T_{eva}$ ($^0$C) | COP | ETA-II | EDR |
|---|---|---|---|
| -15 | 2.192 | 0.3398 | 4.412 |
| -10 | 3.327 | 0.4427 | 2.229 |
| -5 | 4.044 | 0.4527 | 1.935 |
| 0 | 4.746 | 0.4346 | 1.915 |
| 5 | 5.595 | 0.4026 | 2.025 |
| 10 | 6.715 | 0.3659 | 2.301 |

**Table 2: Variation of Performance Parameters with Evaporator Temperature in the Vapour Compression Refrigeration System using R-407c in Primary Circuit and Titanium Dioxide Nonoparticles of 10 Micron Particle's Diameter in Secondary Circuit for Condenser Temperature 48oc**

| $T_{eva}$ ($^0$C) | COP | ETA-II | EDR |
|---|---|---|---|
| -10 | 3.012 | 0.4008 | 2.735 |
| -5 | 4.634 | 0.5158 | 1.458 |
| 0 | 5.67 | 0.5193 | 1.338 |
| 5 | 6.742 | 0.4850 | 1.421 |
| 10 | 8.103 | 0.4295 | 1.656 |

**Table 3: Variation of Performance Parameters with Evaporator Temperature in the Vapour Compression Refrigeration System Using R-134a in Primary Circuit and Titanium Dioxide Nonoparticles of 10 Micron Particle's Diameter in Secondary Circuit for Condenser Temperature 48oc**

| $T_{eva}$($^0$C) | COP | ETA-II | EDR |
|---|---|---|---|
| -10 | 2.182 | 0.2904 | 5.356 |
| -5 | 4.36 | 0.4880 | 1.659 |
| 0 | 5.517 | 0.5052 | 1.418 |
| 5 | 6.595 | 0.4744 | 1.484 |
| 10 | 7.932 | 0.4204 | 1.722 |

**Table 4: Variation of Performance Parameters with Evaporator Temperature in the Vapour Compression Refrigeration System Using R-410a in Primary Circuit and Titanium Dioxide Nonoparticles of 10 Micron Particle's Diameter in Secondary Circuit for Condenser Temperature 48oc**

| $T_{eva}$($^0$C) | COP | ETA-II | EDR |
|---|---|---|---|
| -15 | 1.466 | 0.2274 | 12.83 |
| -10 | 1.932 | 0.2571 | 7.065 |
| -5 | 2.138 | 0.2394 | 6.847 |
| 0 | 2.282 | 0.2089 | 7.52 |
| 5 | 2.416 | 0.2738 | 8.816 |
| 10 | 2.557 | 0.1355 | 11.12 |

**Table 5: Variation of Performance Parameters with Condenser Temperature in the Vapour Compression Refrigeration System Using R-502 in Primary Circuit and Titanium Dioxide Nonoparticles Of 10 Micron Particle's Diameter in Secondary Circuit for Condenser Temperature 48oc**

| $T_{eva}$($^0$C) | COP | ETA-II | EDR |
|---|---|---|---|
| -15 | 2.769 | 0.4294 | 2.645 |
| -10 | 3.908 | 0.5201 | 1.584 |
| -5 | 4.671 | 0.5229 | 1.433 |
| 0 | 5.448 | 0.4489 | 1.455 |
| 5 | 6.396 | 0.4601 | 1.576 |
| 10 | 7.645 | 0.4052 | 1.839 |

**Table 6:Variation of Performance Parameters with Evaporator Temperature in the Vapour Compression Refrigeration System Using R-404a in Primary Circuit and Titanium Dioxide Nonoparticles of 10 Micron Particle's Diameter in Secondary Circuit for Condenser Temperature 48oc**

| $T_{eva}(^0C)$ | COP | ETA-II | EDR |
|---|---|---|---|
| -15 | 2.242 | 0.3477 | 2.242 |
| -10 | 3.525 | 0.4691 | 3.525 |
| -5 | 4.303 | 0.4817 | 4.303 |
| 0 | 5.048 | 0.4663 | 5.048 |
| 5 | 5.942 | 0.4275 | 5.942 |
| 10 | 7.12 | 0.3774 | 7.12 |

**Table 7: Variation of Performance Parameters with Evaporator Temperature in the Vapour Compression Refrigeration System Using R-152a in Primary Circuit and Titanium Dioxide Nonoparticles of 10 Micron Particle's Diameter in Secondary Circuit for Condenser Temperature 48oc**

| $T_{eva}(^0C)$ | COP | ETA-II | EDR |
|---|---|---|---|
| -10 | 2.70 | 0.3593 | 3.42 |
| -5 | 5.164 | 0.5786 | 1.143 |
| 0 | 6.493 | 0.5946 | 0.9880 |
| 5 | 7.734 | o.5564 | 1.064 |
| 10 | 9.273 | 0.4917 | 1.281 |

**Table 8: Variation of Performance Parameters with Condenser Temperature in the Vapour Compression Refrigeration System Using R-507a in Primary Circuit and Titanium Dioxide Nonoparticles of 10 Micron Particle's Diameter in Secondary Circuit for Condenser Temperature 48oc**

| $T_{eva}(^0C)$ | COP | ETA-II | EDR |
|---|---|---|---|
| -15 | 2.399 | 0.3719 | 3.611 |
| -10 | 3.58 | 0.4765 | 1.920 |
| -5 | 4.328 | 0.4844 | 1.685 |
| 0 | 5.06 | 0.4634 | 1.689 |
| 5 | 5.945 | 0.4277 | 1.811 |
| 10 | 7.09 | 0.3768 | 2.088 |

**Table 9: Variation of Performance Parameters with Evaporator Temperature in the Vapour Compression Refrigeration System Using R-290 in Primary Circuit and Titanium Dioxide Nonoparticles of 10 Micron Particle's Diameter in Secondary Circuit for Condenser Temperature 48oc**

| $T_{EVA}(^oC)$ | COP | ETA II | EDR |
|---|---|---|---|
| -15 | 3.043 | 0.4717 | 2.158 |
| -10 | 4.046 | 0.5437 | 1.435 |
| -5 | 4.826 | 0.5402 | 1.335 |
| 0 | 5.599 | 0.5127 | 1.374 |
| 5 | 6.548 | 0.4711 | 1.505 |
| 10 | 7.802 | 0.4135 | 1.774 |

**Table 10: Variation of Performance Parameters with Evaporator Temperature in the Vapour Compression Refrigeration System Using R-600a in Primary Circuit and Titanium Dioxide Nonoparticles of 10 Micron Particle's Diameter in Secondary Circuit for Condenser Temperature 48oc**

| $T_{EVA}(^oC)$ | COP | ETA II | EDR |
|---|---|---|---|
| -15 | -------- | ------- | ------- |
| -10 | 2.588 | 0.3444 | 3.733 |
| -5 | 4.009 | 0.4488 | 1.969 |
| 0 | 4.873 | 0.4462 | 1.82 |
| 5 | 5.751 | 0.4137 | 1.926 |
| 10 | 6.866 | 0.3639 | 2.216 |

**Table 11: Variation of Performance Parameters with Evaporator Temperature in the Vapour Compression Refrigeration System Using R-600 in Primary Circuit and Titanium Dioxide Nonoparticles of 10 Micron Particle's Diameter in Secondary Circuit for Condenser Temperature 48oc**

| $T_{EVA}(^oC)$ | COP | ETA II | EDR |
|---|---|---|---|
| -15 | ------- | ------- | ------- |
| -10 | ------- | ------- | ------- |
| -5 | 3.605 | 0.4036 | 2.429 |
| 0 | 4.922 | 0.4507 | 1.784 |
| 5 | 5.932 | 0.4267 | 1.818 |
| 10 | 7.122 | 0.3775 | 2.082 |

**Table 12: Variation of Performance Parameters with Evaporator Temperature in the Vapour Compression Refrigeration System Using R-290 in Primary Circuit and Titanium Dioxide Nonoparticles of 10 Micron Particle's Diameter in Secondary Circuit for Condenser Temperature 48oc**

| $T_{EVA}$(°C) | COP | ETA II | EDR |
|---|---|---|---|
| -15 | 3.043 | 0.4717 | 2.158 |
| -10 | 4.046 | 0.5437 | 1.435 |
| -5 | 4.826 | 0.5402 | 1.335 |
| 0 | 5.599 | 0.5127 | 1.374 |
| 5 | 6.548 | 0.4711 | 1.505 |
| 10 | 7.802 | 0.4135 | 1.774 |

**Table 13: Variation of Performance Parameters with Condenser Temperature in the Vapour Compression Refrigeration System Using R-125 in Primary Circuit and Titanium Dioxide Nonoparticles of 10 Micron Particle's Diameter in Secondary Circuit for Evaporator Temperature - 5oc**

| $T_{cond}$ ($^0$C) | COP | ETA-II | EDR |
|---|---|---|---|
| 40 | 5.26 | 0.5888 | 1.097 |
| 44 | 4.605 | 0.5155 | 1.478 |
| 48 | 4.044 | 0.4527 | 1.935 |
| 52 | 3.532 | 0.3953 | 2.529 |
| 56 | 3.025 | 0.3386 | 3.411 |

**Table 14: Variation of Performance Parameters with Condenser Temperature in the Vapour Compression Refrigeration System Using R-407c in Primary Circuit and Titanium Dioxide Nonoparticles Of 10 Micron Particle's Diameter in Secondary Circuit for Evaporator Temperature - 5oc**

| $T_{Cond}$ ($^0$C) | COP | ETA-II | EDR |
|---|---|---|---|
| 40 | 6.339 | 0.7096 | 0.6732 |
| 44 | 5.462 | 0.6114 | 1.002 |
| 48 | 4.634 | 0.5148 | 1.458 |
| 52 | 3.738 | 0.4185 | 2.262 |

**Table 15. Variation of Performance Parameters with Condenser Temperature in the Vapour Compression Refrigeration System Using R-134a in Primary Circuit and Titanium Dioxide Nonoparticles of 10 Micron Particle's Diameter in Secondary Circuit for Evaporator Temperature - 5oc**

| $T_{cond}$($^0$C) | COP | ETA-II | EDR |
|---|---|---|---|
| 40 | 6.096 | 0.6824 | 0.7531 |
| 44 | 5.229 | 0.5854 | 1.112 |
| 48 | 4.36 | 0.4880 | 1.659 |
| 52 | 3.342 | 0.3741 | 2.814 |
| 56 | 1.992 | 0.2230 | 8.004 |

**Table 16: Variation of Performance Parameters with Evaporator Temperature in the Vapour Compression Refrigeration System Using R-502 in Primary Circuit and Titanium Dioxide Nonoparticles of 10 Micron Particle's Diameter in Secondary Circuit for Evaporator Temperature - 5oc**

| $T_{cond}$($^0$C) | COP | ETA-II | EDR |
|---|---|---|---|
| 40 | 6.035 | 0.6753 | 0.7749 |
| 44 | 5.294 | 0.5927 | 1.08 |
| 48 | 4.671 | 0.5229 | 1.437 |
| 52 | 4.118 | 0.4610 | 1.865 |
| 56 | 3.591 | 0.4019 | 2.448 |

**Table 17: Variation of Performance Parameters with Condenser Temperature in the Vapour Compression Refrigeration System Using R-410a in Primary Circuit and Titanium Dioxide Nonoparticles of 10 Micron Particle's Diameter in Secondary Circuit**

| $T_{cond}$($^0$C) | COP | ETA-II | EDR |
|---|---|---|---|
| 40 | 2.183 | 0.2443 | 6.554 |
| 44 | 2.166 | 0.2425 | 6.66 |
| 48 | 2.138 | 0.2394 | 6.847 |
| 52 | 2.087 | 0.2337 | 7.215 |
| 56 | 1.99 | 0.2228 | 8.02 |

**Table 18: Variation of Performance Parameters with Condenser Temperature in the Vapour Compression Refrigeration System Using R-404a in Primary Circuit and Titanium Dioxide Nonoparticles of 10 Micron Particle's Diameter in Secondary Circuit for Evaporator Temperature - 5oc**

| $T_{cond}$($^0$C) | COP | ETA-II | EDR |
|---|---|---|---|
| 40 | 5.603 | 0.6272 | 0.9408 |
| 44 | 4.903 | 0.5489 | 1.289 |
| 48 | 4.303 | 0.4817 | 1.704 |
| 52 | 3.754 | 0.4202 | 2.2244 |
| 56 | 3.205 | 0.3588 | 3.051 |

**Table 19: Variation of Performance Parameters with Condenser Temperature in the Vapour Compression Refrigeration System Using R-152a in Primary Circuit and Titanium Dioxide Nonoparticles of 10 Micron Particle's Diameter in Secondary Circuit for Evaporator Temperature - 5oc**

| $T_{cond}$($^0$C) | COP | ETA-II | EDR |
|---|---|---|---|
| 40 | 7.207 | 0.8067 | 0.4393 |
| 44 | 6.185 | 0.6923 | 0.7229 |
| 48 | 5.169 | 0.5786 | 1.143 |
| 52 | 3.99 | 0.4467 | 1.987 |
| 56 | 2.434 | 0.2725 | 5.228 |

**Table 20: Variation of Performance Parameters with Condenser Temperature in the Vapour Compression Refrigeration System Using R-507a in Primary Circuit and Titanium Dioxide Nonoparticles of 10 Micron Particle's Diameter in Secondary Circuit for Evaporator Temperature - 5oc**

| Tcond(0C) | COP | ETA-II | EDR |
|---|---|---|---|
| 40 | 5.62 | 0.6291 | 0.9335 |
| 44 | 4.924 | 0.5512 | 1.277 |
| 48 | 4.328 | 0.4844 | 1.685 |
| 52 | 3.785 | 0.4237 | 2.208 |
| 56 | 3.249 | 0.3636 | 2.973 |

**Table 21: Variation of Performance Parameters with Condenserr Temperature in the Vapour Compression Refrigeration System Using R-290 in Primary Circuit and Titanium Dioxide Nonoparticles of 10 Micron Particle's Diameter in Secondary Circuit for Evaporator Temperature - 5oc**

| $T_{cond}$($^o$C) | COP | ETA II | EDR |
|---|---|---|---|
| 40 | 6.18 | 0.6918 | 0.7246 |
| 44 | 5,444 | 0.6094 | 1.01 |
| 48 | 4.826 | 0.5402 | 1.335 |
| 52 | 4.281 | 0.4792 | 1.723 |
| 56 | 3.768 | 0.4278 | 2.227 |

**Table 22: Variation of Performance Parameters with Condenser Temperature in the Vapour Compression Refrigeration System Using R-600a in Primary Circuit and Titanium Dioxide Nonoparticles of 10 Micron Particle's Diameter in Secondary Circuit for Evaporator Temperature - 5oc**

| $T_{cond}$($^o$C) | COP | ETA II | EDR |
|---|---|---|---|
| 40 | 5.377 | 0.6019 | 1.041 |
| 44 | 4.672 | 0.5230 | 1.433 |
| 48 | 4.009 | 0.4488 | 1.969 |
| 52 | 3.297 | 0.3690 | 2.89 |
| 56 | 2.423 | 0.2712 | 5.279 |

**Table 23: Variation of Performance Parameters with Condenser Temperature in the Vapour Compression Refrigeration System Using R-600 in Primary Circuit and Titanium Dioxide Nonoparticles of 10 Micron Particle's Diameter in Secondary Circuit for Evaporator Temperature - 5oc**

| $T_{cond}$($^o$C) | COP | ETA II | EDR |
|---|---|---|---|
| 40 | 5.446 | 0.6096 | 1.009 |
| 44 | 4.578 | 0.5125 | 1.497 |
| 48 | 3.605 | 0.4036 | 2.429 |
| 52 | 2.323 | 0.260 | 5.754 |
| 56 | 1.484 | 0.1661 | 17.47 |

**Table 24: Variation of Performance Parameters with Condenser Temperature in the Vapour Compression Refrigeration System Using R-290 in Primary Circuit and Titanium Dioxide Nonoparticles of 10 Micron Particle's Diameter in Secondary Circuit for Evaporator Temperature - 5oc**

| $T_{cond}$(°C) | COP | ETA II | EDR |
|---|---|---|---|
| 40 | 6.18 | 0.6918 | 0.7246 |
| 44 | 5,444 | 0.6094 | 1.01 |
| 48 | 4.826 | 0.5402 | 1.335 |
| 52 | 4.281 | 0.4792 | 1.723 |
| 56 | 3.768 | 0.4278 | 2.227 |

**4.0 Conclusions**

The performances of vapour compression have been studies in details and following conclusions were made.

1 The optimum temperature of evaporator is found to be -5oC. Similarly exergy destruction ratio is also decreases up to 273K and then increases. The optimum evaporator temperature to be found to be 273K for optimum EDR condenser temperature with performance parameters.

2 As condenser temperature increases, the first law efficiency of vapour compression refrigeration system is decreases. Also second law efficiency is also decreases. Similarly exergy destruction ratio is also decreases.

3 Use of nano particle suspended in the water used as refrigerant in the secondary circulit in the evaporator greatly affecting its first law performance.

4 As evaporator temperature is increases, the first law efficiency and second law efficiency increases.

The increasing condenser temperature the First law and second law performance decreases

**References**

[1] Johnson. E. Global warming from HFC. Environ. Impact Asses.1998; 18 485-492.

[2] Qiyu Chen, R.C Prasad. Simulation of a vapour compression refrigeration cycles HFC134A and CFC12.Int Comm.Heat Mass Transfer.1999; 26 513-521.

[3] M. Padilla, R. Revellin, J. Bonjour. Exergy analysis of R413A as replacement of R12 in a domestic refrigeration system. Int J Energy Conversion and Management.2010; 51 2195-2201.

[4] H.O. Spauschus. HFC 134a as a substitute refrigerant for CFC 12. Int J of Refrigeration. 1988; 11 389-392.

[5] J. U. Ahamed, R. Saidur, H. H. Masjuki, A review on exergy analysis of vapor compression refrigeration system. Int J Renewable and sustainable energy reviews.2011; 15 1593-1600.

[6] R. Llopis, E. Torrella, R. Cabello, D. Sánchez. Performance evaluation of R404A and R507A refrigerant mixtures in an experimental double-stage of vapour compression plant. Int J Applied Energy.2010; 87 1546-1553.

[7] Akhilesh Arora, S. C. Kaushik. Theoretical analysis of a vapour compression refrigeration system with R502, R404A and R507A. Int J Refrigeration.2008; 31 998-1005.

[8] V. Havelsky. Investigation of refrigerating system with R12 refrigerant replacements .Int J Applied Thermal Engineering.2000; 20 133-140.

[9] V. Siva Reddy, N. L Panwar, S. C Kaushik-Exergy analysis of a vapour compression refrigeration system with R134a,R143a,R152a,R404A,R407C,R410A,

R502 and R507A.Clean Techn Environ Policy.2012;14 47-53.

[10] R. Saravanakumar, V. Selladurai-Exergy analysis of a domestic refrigerator using eco-friendly R290/R600a refrigerant mixture as an alternative to R134a.Int J Therm Anal Calorim.2013

[11] C. Nikolaidis, D. Probert-Exergy method analysis of a two-stage vapour-compression refrigeration-plants performance. Int J Applied Thermal Engineering.1998; 60 241-256.

[12] S. Kumar, M. Prevost, R. Bugarel- Exergy analysis of a vapour compression refrigeration system. Heat Recovery Systems & CHP.1989; 9 151-157.

[13] Mahmood Mastani Joybari, Mohammad Sadegh Hatamipour, Amir Rahimi, Fatemeh Ghadiri Modarres- Exergy analysis and optimization of R600a as a replacement of R134a in a domestic refrigerator system. International Journal of refrigeration.2013; 36 1233-1242.

[14] S. Anand, S. K Tyagi-Exergy analysis and experimental study of a vapour compression refrigeration cycle.Int J Therm Anal Calorim.2012; 110 961-971.

[15] J. U Ahamed, R. saidur, H. H Masjuki, M. A Sattar- An analysis of energy, exergy and sustainable development of a vapour compression refrigeration system using hydrocarbon.International journal of Green energy.2012; 9 707-717.

[16] Camelia Stanciu, Adina Gheorghian, Dorin Stanciu, Alexandru Dobrovicescu- Exergy analysis and refrigerant effect on the operation and performance lomits of a one stage vapour compression refrigeration system.Termotehnica.2011;1 36-42.

[17] J. U. Ahamed, R. Saidur, H. H. Masjuki. A review on exergy analysis of vapor compression refrigeration system. Int J Renewable and sustainable energy reviews.2011; 15 1593-1600.

[18] B. O. Bolaji, M. A. Akintunde, T. O. Falade. Comparative analysis of performance of three ozone-friends HFC refrigerants in a vapor compression refrigerator. Int J Sustainable Energy & Environment.2011; 2 61-64.

[19] Recep Yumrutas, Mehmet Kunduz, Mehmet Kanoglu-Exergy analysis of vapor compression refrigeration systems. Exergy, An International Journal.2002; 2 266-272.

[20] M. Padilla, R. Revellin, J. Bonjour. Exergy analysis of R413A as replacement of R12 in a domestic refrigeration system. Int J Energy Conversion and Management.2010; 51 2195-2201.

[21] H. M Getu, P. K Bansal. Thermodynamic analysis of an R744-R717 cascade refrigeration system. Int J Refrigeration.2008; 31 45-54.

[22] Mark W. Spatz, Samuel F. Yana Motta. An evaluation of options for replacing HCFC-22 in medium temperature refrigeration systems. Int J Refrigeration.2004; 27 475-483.

[23] M. Mohanraj, S. Jayaraj, C. Muraleedharan, P. Chandrasekar.Experimental investigation of R290/R600a mixture as an alternative to R134a in a domestic refrigerator. Int J Thermal Sciences.2009; 48 1036-1042.

[24] X. H. Han, Q. Wang, Z.W. Zhu, G.M. Chen. Cycle performance study on R32/R125/R161 as an alternative refrigerant to R407C. Int J Applied Thermal Engineering.2007; 27 2559-2565.

[25] E. Halimic, D. Ross, B. Agnew, A. Anderson, I. Potts. A comparison of the operating performance of alternative refrigerants. Int J Applied Thermal Engineering.2003; 23 1441-1451.

[26] Yongmei Xuan, Guangming Chen. Experimental study on HFC-161 mixture as

an alternative refrigerant to R502. Int J Refrigeration. Article in Press.

[27] R. Cabello, J. Navarro-Esbrı, R. Llopis, E. Torrella. Analyses of the variation mechanism in the main energetic parameters in a single-stage vapour compression plant. Int J Applied Thermal Engineering.2007; 27 167-176.

[28] R. Cabello, E. Torrella, J. Navarro-Esbr. Experimental evaluation of a vapour compression plant performance using R134a, R407C and R22 as working fluids. Int J Applied Thermal Engineering.2004; 24 1905-1917.

[29] Klein, S. A., AlvaradoF. Engineering Equation Solver, Version 7.441. F Chart Software, Middleton, WI.2005.

[30] Dincer. I. Refrigeration Systems and Applications. Wiley, UK.2003 26.

[31] Elcock D. Potential impacts of nanotechnology on energy transmission applications and needs. Environmental Science Division, Argonne National Laboratory; 2007.

[32] Hindawi, Special issue on heat transfer in nanofluids; 2009

[33] Eastman JA, Choi US, Thompson LJ, Lee S. Enhanced thermal conductivity through the development of nanofluids. Mater Res Soc Symp Proc 1996;457 3–11.

[34] Liu MS, Lin MCC, Huang IT, Wang CC. Enhancement of thermal conductivity with CuO for Nanofluids. Chemical Engineering and Technology 2006; 29(1) 72–7.

[35] Jiang W, Ding G, Peng H. Measurement and model on thermal conductivities of carbon nanotube nanorefrigerants. International Journal of Thermal Sciences 2009;48 1108–15

[36] Hwang YJ, Ahn YC, Shin HS, Lee CG, Kim GT, Park HS, et al. Investigation on characteristics of thermal conductivity enhancement of nanofluids. Current Applied Physics 2006; 6(6) 1068–71.

[37] Yoo D-H, Hong KS, Yang H-S. Study of thermal conductivity of nanofluids for the application of heat transfer fluids. Thermochimica Acta 2007; 455(1–2) 66–9.

[38] Choi SUS, Zhang ZG, Yu W, Lockwood FE, Grulke EA. Anomalous thermal conductivity enhancement in nanotube suspensions. Applied Physics Letters 2001; 79(14) 2252–4.

[39] Yang Y. Carbon nanofluids for lubricant application. University of Kentucky; 2006.

[40] Eastman JA, Choi SUS, Li S, Yu W, Thompson LJ. Anomalously increased effective thermal conductivities of ethylene glycol-based nanofluids containing copper nanoparticles. Applied Physics Letters 2001; 78(6) 718–20.

[41] Yang Y. Carbon nanofluids for lubricant application. University of Kentucky;2006

[42] Kang HU, Kim SH, Oh JM. Estimation of thermal conductivity of nanofluid using experimental effective particle. Experimental Heat Transfer 2006; 19(3) 181–91.

[43] Lee J-H, Hwang KS, Jang SP, Lee BH, Kim JH, Choi SUS, et al. Effective viscosities and thermal conductivities of aqueous nanofluids containing low volume concentrations of Al2O3 nanoparticles. International Journal of Heat and Mass Transfer 2008; 51(11–12) 2651–6.

[44] Jiang W, Ding G, Peng H. Measurement and model on thermal conductivities of carbon nanotube nanorefrigerants. International Journal of Thermal Sciences 2009; 48 1108–15.

[45] Wu XM, Li P, Li H, Wang WC. Investigation of pool boiling heat transfer of R11 with TiO2 nano-particles. Journal of Engineering Thermophysics 2008; 29(1) 124–6.

[46] Trisaksri V, Wongwises S. Nucleate pool boiling heat transfer of TiO2–R141b nanofluids. International Journal of Heat and Mass Transfer 2009; 52(5–6) 1582–8.

[47] Hao P, Guoliang D, Weiting J, Haitao H, Yifeng G. Heat transfer characteristics of refrigerant-based nanofluid flow boiling inside a horizontal smooth tube. International Journal of Refrigeration 2009; 32 1259–70.

[48] Hao P, Guoliang D, Haitao H, Weiting J, Dawei Z, Kaijiang W. Nucleate pool boiling heat transfer characteristics of refrigerant/oil mixture with diamond nanoparticles. International Journal of refrigeration 2010; 33 347–58.

[49] Wang KJ, Ding GL, Jiang WT. Nano-scale thermal transporting and its use in engineering. In Proceedings of the 4th symposium on refrigeration and air condition; 2006, 66–75.

[50] Li P, Wu XM, Li H. Pool boiling heat transfer experiments of refrigerants with nanoparticle TiO2. In Proceedings of the 12th symposium on engineering thermophysics; 2006, 325–8.

[51] Peng H, Ding G, Jiang W, Hu H, Gao Y. Heat transfer characteristics of refrigerant-based nanofluid flow boiling inside a horizontal smooth tube.International Journal of Refrigeration; 2009;32 1259–70.

[52] D.Sendil Kumar, R. Elansezhian.Zno nanorefrigerant in R152a refrigeration system for energy conservation and green environment.J Front Mech Engg ; 2014;1-6.

[53] I. M. Mahbubul, S. A. Fadhilah, R. Saidur, K. Y. Leong, M. A. Amalina, Thermophysical properties and heat transfer performance of Al2O3/R-134a nanorefrigerants.International Journal of Heat and Mass Transfer ;2013;57 100–108s.